Scientific Research Publishing

Open Journal of Applied Sciences, 2022, 12, 1770-1782
https://www.scirp.org/journal/ojapps
ISSN Online: 2165-3925
ISSN Print: 2165-3917

Thermal Performance and Emission Analysis of a New Model Cylindrical Cook Stove with Controlled Air Flow

Issaka Ouédraogo[1*], Bouwèreou Bignan-Kagomna[2], W. D. Arsène Ilboudo[1], Albert Keré[3]

[1]Research Institute in Applied Sciences and Technology/National Scientific and Technological Research Center, Ouagadougou, Burkina Faso
[2]Thermal and Renewable Energy Laboratory, Joseph Ki Zerbo University, Ouagadougou, Burkina Faso
[3]Green Innovation Centers Project, Ouagadougou, Burkina Faso
Email: *issaka72ouedraogo@gmail.com

How to cite this paper: Ouédraogo, I., Bignan-Kagomna, B., Ilboudo, W.D.A. and Keré, A. (2022) Thermal Performance and Emission Analysis of a New Model Cylindrical Cook Stove with Controlled Air Flow. *Open Journal of Applied Sciences*, **12**, 1770-1782.
https://doi.org/10.4236/ojapps.2022.1211122

Received: September 29, 2022
Accepted: November 4, 2022
Published: November 7, 2022

Abstract

We present in this paper the results of experimental and numerical study of the thermal performances of a cook stove prototype intended for the parboiling of paddy rice. Thus, the experimental results show that the optimal mass of husk rice is M = 7.15 kg for a good combustion within the combustion chamber and got a maximum temperature at the level of the burners surface. This temperature is $T_{cu_1} = 304.78^{\circ}\mathrm{C}$. The circulating air flow rate by forced convection is Q_m = 0.09112 $m^{-3}{\cdot}s^{-1}$. The vertical side walls temperature is T_{ple} = 140.6˚C and the water temperature and vapor is about 144.6˚C in the stockpot. The gas combustion is composed of carbon dioxide (CO_2), carbon monoxide (CO), methane (CH_4) and the ratio of hydrogen to nitrogen (H_2/N_2). The results from the numerical modeling indicate $T_{cu_1} = 307.8^{\circ}\mathrm{C}$, T_{ple} = 144.55˚C and a Q_m = 0.09258 $m^{-3}.s^{-1}$. The average thermal efficiency of the cookstove is η = 46.6% and the power developed by the cookstove is about ≈6 kW. Despite the heat losses, the cookstove remains interesting for paddy rice parboiling activities.

Keywords

Cookstove, Thermal Performance, Emissions

1. Introduction

Wood fuels are the main sources of energy in the country. Indeed, wood and charcoal account for 85% of the country's energy consumption, and cover about

95% of domestic needs [1] [2] [3]. The high consumption of wood contributes to an imbalance in the supply and demand of fuel wood. The result is an ecological, economic and social crisis in rural and urban areas. In view of these different crises, the problem of firewood has been posed a concern for rural development and energy [4] [5] [6] [7]. Thus, substitution strategies are put in place to reduce the consumption of wood. It is in this perspective that we are interested in the technologies of paddy rice parboiling.

Most paddy rice parboiling centers in Burkina Faso use wood as an energy source to process paddy rice. According to the National Union of Rice Parboilers of Burkina, approximately 7.350 carts, or the equivalent of 2.756.43 tons of wood, were used for rice parboiling by member associations of the structure in 2015 [8] [9]. As a reminder, rice parboiling is a technique that consists of vapor treatment at high temperature, the objective of which is to weaken the husk of the rice grains. This process significantly increases the quality of rice and improves its nutritional elements.

Thus, several technologies for replacing wood with rice husk have been developed. Rice husk ovens have been developed rapidly in paddy parboiling centers. It was found that about 100% of women processors have adopted rice husks as a source of fuel in paddy rice processing centers [10] [11] [12] [13]. Although paddy rice processors report feelings of satisfaction, these rice husk cook stoves have low thermal efficiencies, estimated at 25% - 30%, and energy losses of over 50% [14] [15]. Rice husk consumption ratios show that thermally, these cook stoves are not very efficient. Finally, we propose to study experimentally and numerically the thermal performance of a new prototype of cook stove for paddy rice parboiling.

2. Cook Stove Description

The cook stove is represented by the **Figure 1**. It is composed of black steel and two parts. The upper part, which constitutes the burners and the lower part of cylindrical shape that constitutes the combustion chamber. It is also equipped with two side walls and each side wall to a thickness of Ep_1 = 2 mm. The cooker has a thickness of Ep_2 = 3 mm. The combustion chamber has a volume of 1508.3 cm^3, a diameter d = 60 cm and a height H = 55 cm.

The stockpot intended for parboiling paddy rice made of stainless steel plate with a diameter d_{ex} = 73 cm and a volume of 209,269.3 cm^3. The cook stove is equipped with a screw iron support giving it the ability to rotate. A curved channel of shape ensures the circulation of air flow to the combustion chamber. The cook stove is supplied with air flow from a ventilation system, the power is 1840 W. The whole ventilation system is powered by solar photovoltaic panel with a Ws = 275 Wp. The connection mode can be direct or indirect with a storage system of a solar battery with a capacity of 200 Ah. The objective is to ensure an autonomous functioning of the cook stove. The principle of operation of the cook stove to introduce a mass of rice husk into the combustion chamber at

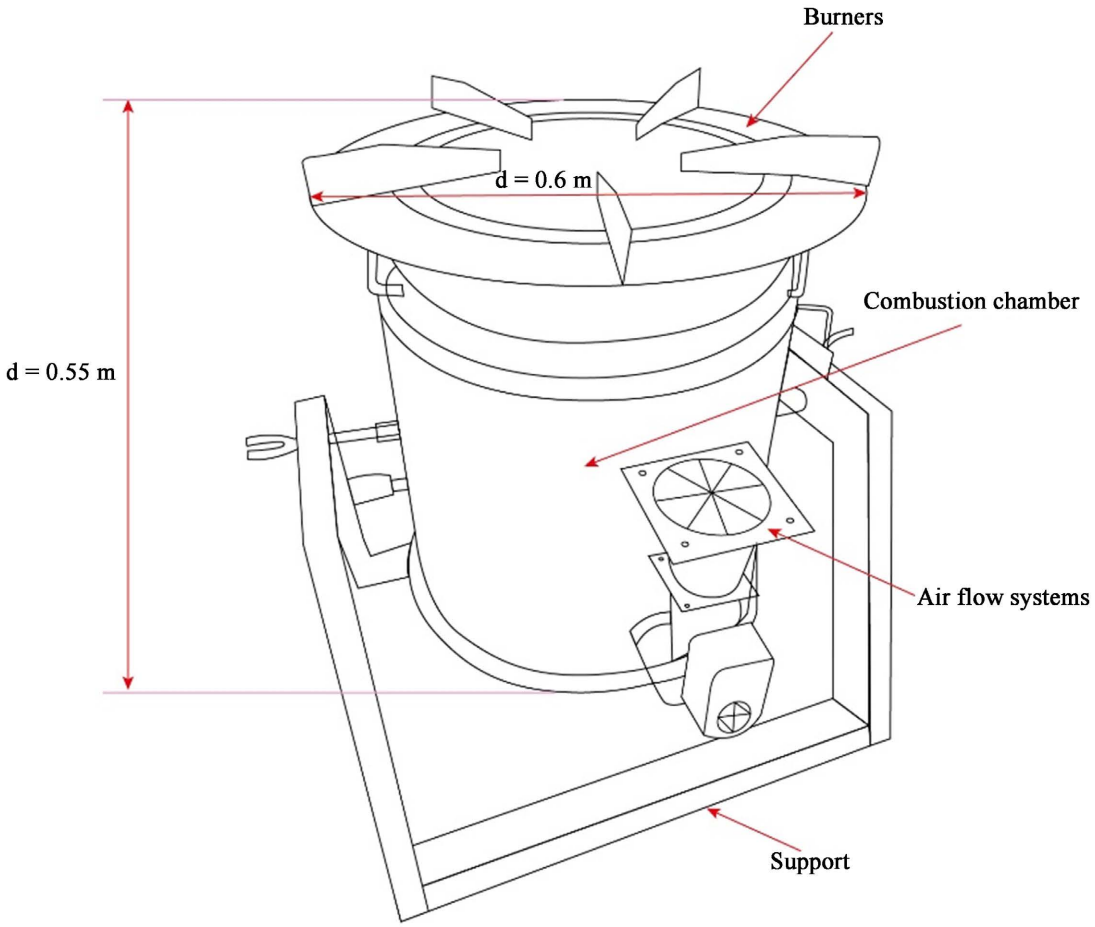

Figure 1. The schema of the cook stoves model studied.

the upper part of the cook stove. Then the combustion chamber is ignited and closed. The ventilation system ensures a variable air flow to the combustion. The air flow is adjusted to maintain a good combustion.

2.1. Mathematical Formulation

The method consists of cutting the cook stove into fictitious sections in the direction of the air flow in the combustion chamber. we emit some assumptions: 1) any mass transfer in the cook stove, 2) circulating air flow is unidirectional, 3) the physical properties of the air and the materials constituting the cook stove are assumed to be constant. To write the heat balances in each section we use analogies which exist between the thermal transfers and the transfers of electricity. The application of the Ohm's law to each section leads to the following heat balances:

Vertical wall surface:

$$\frac{M_{ple}CP_{ple}}{S}\frac{\partial T_{ple}}{\partial t} = \frac{\lambda_{ple}}{Ep_{ple}}\left(T_{pli}-T_{ple}\right)+hc_1\left(T_{amb}-T_{ple}\right)+hr_{amb}\left(T_{amb}-T_{ple}\right) + \sum_{i=1}^{3} hr_{i\to ple}F_{i,t_{ple}}\left(T_i-T_{ple}\right) \quad (1)$$

$$\frac{M_{ple}CP_{ple}}{S}\frac{\partial T_{pli}}{\partial t}=\frac{\lambda_{pli}}{Ep_{pli}}\left(T_{ple}-T_{pli}\right)+hc_2\left(T_a-T_{pli}\right)+hr_{p\to pli}\left(T_{cu_1}-T_{pli}\right)+\sum_{i=1}^{3}hr_{i\to t_{pli}}F_{i,t_{pli}}\left(T_i-T_{pli}\right) \tag{2}$$

The air temperature

$$\frac{M_aCP_a}{S}\frac{\partial T_a}{\partial t}=hc_3\left(T_{cu_2}-T_a\right)+hc_2\left(T_{pli}-T_a\right)+hc_4\left(T_{fon}-T_a\right)+Pu \tag{3}$$

The burner surface:

$$\frac{M_{cu}CP_{cu}}{S}\frac{\partial T_{cu1}}{\partial t}=\frac{\lambda_{cu}}{Ep_{cu}}\left(T_{cu2}-Tcu_1\right)+hr_{ple}\left(T_{mar}-Tcu_1\right)+hc_1\left(T_{amb}-Tcu_1\right)+hr_{amb}\left(T_{amb}-Tcu_1\right) \tag{4}$$

$$\frac{M_{cu}CP_{cu}}{S}\frac{\partial T_{cu_2}}{\partial t}=\frac{\lambda_{cu}}{Ep_{cu}}\left(T_{cu_1}-T_{cu_2}\right)+hr_{ple}\left(T_{ple}-T_{cu_2}\right)+hc_3\left(T_a-T_{cu_2}\right)+hr_{amb}\left(T_{amb}-T_{cu_2}\right) \tag{5}$$

Lower wall surface:

$$\frac{M_{ple}CP_{ple}}{S}\frac{\partial T_{fon}}{\partial t}=\frac{\lambda_{ple}}{Ep_{ple}}\left(T_{pli}-T_{fon}\right)+hr_{pli}\left(T_{pli}-T_{fon}\right)+hc_4\left(T_a-T_{fon}\right) \tag{6}$$

2.2. Equations Discretizations

The (1)-(6) equations are discretized using the implicit finite difference method. As a reminder, knowledge of certain temperatures T_{pli}^{t+1}, T_a^{t+1}, $T_{cu_2}^{t+1}$, T_{fon}^{t+1} within the combustion chamber is necessary. Thus:

Equation (1) becomes:

$$\frac{M_{ple}CP_{ple}}{S}\frac{T_{ple}^{t+1}-T_{ple}^{t}}{\Delta t}=\frac{\lambda_{ple}}{Ep_{ple}}\left(T_{pli}^{t}-T_{ple}^{t}\right)+hc_1\left(T_{amb}^{t}-T_{ple}^{t}\right)+hr_{amb}\left(T_{amb}^{t}-T_{ple}^{t}\right)+hr_{pli}F_{pli,ple}\left(T_{pli}^{t}-T_{ple}^{t}\right)+hr_{amb}F_{amb,ple}\left(T_{amb}^{t}-T_{ple}^{t}\right)+hr_{sol}F_{sol,ple}\left(T_{Sol}^{t}-T_{ple}^{t}\right)$$

$$\begin{aligned}T_{ple}^{t+1}=&\left(1-\frac{\lambda_{ple}S\Delta t}{Ep_{ple}M_{ple}CP_{ple}}-\frac{hc_1S\Delta t}{M_{ple}CP_{ple}}-\frac{hr_{amb}S\Delta t}{M_{ple}CP_{ple}}-\frac{hr_{pli}F_{pli,ple}S\Delta t}{M_{ple}CP_{ple}}-\frac{hr_{amb}F_{amb,ple}S\Delta t}{M_{ple}CP_{ple}}-\frac{hr_{sol}F_{sol,ple}S\Delta t}{M_{ple}CP_{ple}}\right)T_{ple}^{t}\\&+\left(\frac{\lambda_{ple}S\Delta t}{Ep_{ple}M_{ple}CP_{ple}}+\frac{hr_{pli}F_{pli,ple}S\Delta t}{M_{ple}CP_{ple}}\right)T_{pli}^{t}\\&+\left(\frac{hc_1S\Delta t}{M_{ple}CP_{ple}}+\frac{hr_{amb}S\Delta t}{M_{ple}CP_{ple}}+\frac{hr_{amb}F_{amb,ple}S\Delta t}{M_{ple}CP_{ple}}\right)T_{amb}^{t}\\&+\frac{hr_{sol}F_{sol,ple}S\Delta t}{M_{ple}CP_{ple}}T_{Sol}^{t}\end{aligned} \tag{7}$$

Equation (2) becomes:

$$\frac{M_{ple}CP_{ple}}{S}\frac{T_{pli}^{t+1}-T_{pli}^{t}}{\Delta t}=\frac{\lambda_{pli}}{Ep_{pli}}\left(T_{ple}^{t}-T_{pli}^{t}\right)+hc_2\left(T_{a}^{t}-T_{pli}^{t}\right)+hr_{pli}\left(T_{cu1}^{t}-T_{pli}^{t}\right)$$
$$+hr_{ple}F_{ple,pli}\left(T_{ple}^{t}-T_{pli}^{t}\right)+hr_{cu1}F_{cu1,pli}\left(T_{cu1}^{t}-T_{pli}^{t}\right)$$
$$+hr_{sol}F_{sol,pli}\left(T_{Sol}^{t}-T_{pli}^{t}\right)$$

$$T_{pli}^{t+1}=\left(1-\frac{\lambda_{pli}S\Delta t}{Ep_{pli}M_{ple}CP_{ple}}-\frac{hc_2S\Delta t}{M_{ple}CP_{ple}}-\frac{hr_{pli}S\Delta t}{M_{ple}CP_{ple}}\right.$$
$$\left.-\frac{hr_{ple}F_{ple,pli}S\Delta t}{M_{ple}CP_{ple}}-\frac{hr_{cu1}F_{cu1,pli}S\Delta t}{M_{ple}CP_{ple}}-\frac{hr_{sol}F_{sol,pli}S\Delta t}{M_{ple}CP_{ple}}\right)T_{pli}^{t}$$
$$+\left(\frac{\lambda_{ple}S\Delta t}{Ep_{ple}M_{ple}CP_{ple}}+\frac{hr_{ple}F_{ple,pli}S\Delta t}{M_{ple}CP_{ple}}\right)T_{ple}^{t}$$
$$+\frac{hc_2S\Delta t}{M_{ple}CP_{ple}}T_{a}^{t}+\left(\frac{hr_{cu2}S\Delta t}{M_{ple}CP_{ple}}+\frac{hr_{cu2}F_{cu2,pli}S\Delta t}{M_{ple}CP_{ple}}\right)T_{cu2}^{t}$$
$$+\frac{hr_{sol}F_{sol,pli}S\Delta t}{M_{ple}CP_{ple}}T_{Sol}^{t} \tag{8}$$

Equation (3) becomes:

$$\frac{M_aCP_a}{S}\frac{T_{a}^{t+1}-T_{a}^{t}}{\Delta t}=hc_3\left(T_{cu2}^{t}-T_{a}^{t}\right)+hc_2\left(T_{pli}^{t}-T_{a}^{t}\right)+hc_4\left(T_{fon}^{t}-T_{a}^{t}\right)+Pu$$

$$T_{a}^{t+1}=\left(1-\frac{hc_3S\Delta t}{M_aCP_a}-\frac{hc_2S\Delta t}{M_aCP_a}-\frac{hc_4S\Delta t}{M_aCP_a}\right)T_{a}^{t}+\frac{hc_3S\Delta t}{M_aCP_a}T_{cu2}^{t}$$
$$+\frac{hc_2S\Delta t}{M_aCP_a}T_{pli}^{t}+\frac{hc_4S\Delta t}{M_aCP_a}T_{fon}^{t}+\frac{PuS\Delta t}{M_aCP_a} \tag{9}$$

Equation (4) becomes:

$$\frac{M_{cu}CP_{cu}}{S}\frac{T_{cu1}^{t+1}-T_{cu1}^{t}}{\Delta t}=\frac{\lambda_{cu}}{Ep_{cu}}\left(T_{cu2}^{t}-T_{cu1}^{t}\right)+hr_{ple}\left(T_{mar}^{t}-T_{cu1}^{t}\right)$$
$$+hc_1\left(T_{amb}^{t}-T_{cu1}^{t}\right)+hr_{amb}\left(T_{amb}^{t}-T_{cu1}^{t}\right)$$

$$T_{cu1}^{t+1}=\left(1-\frac{\lambda_{cu}S\Delta t}{Ep_{cu}M_{cu}CP_{cu}}-\frac{hr_{ple}S\Delta t}{M_{cu}CP_{cu}}-\frac{hc_1S\Delta t}{M_{cu}CP_{cu}}-\frac{hr_{amb}S\Delta t}{M_{cu}CP_{cu}}\right)T_{cu1}^{t}$$
$$+\frac{\lambda_{cu}S\Delta t}{Ep_{cu}M_{cu}CP_{cu}}T_{cu2}^{t}+\frac{hr_{ple}S\Delta t}{M_{cu}CP_{cu}}T_{mar}^{t}+\left(\frac{hc_1S\Delta t}{M_{cu}CP_{cu}}+\frac{hr_{amb}S\Delta t}{M_{cu}CP_{cu}}\right)T_{amb}^{t} \tag{10}$$

Equation (5) becomes:

$$\frac{M_{cu}CP_{cu}}{S}\frac{T_{cu2}^{t+1}-T_{cu2}^{t}}{\Delta t}=\frac{\lambda_{cu}}{Ep_{cu}}\left(T_{cu1}^{t}-T_{cu2}^{t}\right)+hr_{ple}\left(T_{ple}^{t}-T_{cu2}^{t}\right)$$
$$+hc_3\left(T_{a}^{t}-T_{cu2}^{t}\right)+hr_{amb}\left(T_{amb}^{t}-T_{cu2}^{t}\right)$$

$$T_{cu2}^{t+1}=\left(1-\frac{\lambda_{cu}S\Delta t}{Ep_{cu}M_{cu}CP_{cu}}-\frac{hr_{ple}S\Delta t}{M_{cu}CP_{cu}}-\frac{hc_3S\Delta t}{M_{cu}CP_{cu}}-\frac{hr_{amb}S\Delta t}{M_{cu}CP_{cu}}\right)T_{cu2}^{t}$$
$$+\frac{\lambda_{cu}S\Delta t}{Ep_{cu}M_{cu}CP_{cu}}T_{cu1}^{t}+\frac{hr_{ple}S\Delta t}{M_{cu}CP_{cu}}T_{ple}^{t}+\frac{hc_3S\Delta t}{M_{cu}CP_{cu}}T_{a}^{t}+\frac{hr_{amb}S\Delta t}{M_{cu}CP_{cu}}T_{amb}^{t} \tag{11}$$

Equation (6) becomes:

$$\begin{aligned}
&\frac{M_{ple}CP_{ple}}{S}\frac{T_{fon}^{t+1}-T_{fon}^{t}}{\Delta t}=\frac{\lambda_{ple}}{Ep_{le}}\left(T_{pli}^{t}-T_{fon}^{t}\right)+hr_{pli}\left(T_{pli}^{t}-T_{fon}^{t}\right)+hc_{4}\left(T_{a}^{t}-T_{fon}^{t}\right)\\
&T_{fon}^{t+1}=\left(1-\frac{\lambda_{ple}S\Delta t}{Ep_{ple}M_{ple}CP_{ple}}-\frac{hr_{pli}S\Delta t}{M_{ple}CP_{ple}}-\frac{hc_{4}S\Delta t}{M_{ple}CP_{ple}}\right)T_{fon}^{t}\\
&\quad+\left(\frac{\lambda_{ple}S\Delta t}{Ep_{ple}M_{ple}CP_{ple}}+\frac{hr_{pli}S\Delta t}{M_{ple}CP_{ple}}\right)T_{pli}^{t}+\frac{hc_{4}S\Delta t}{M_{ple}CP_{ple}}T_{a}^{t}
\end{aligned}\tag{12}$$

The air volume flow produced by the forced convection in the channel is calculated by the velocity (V) and by the section (S_0) of the channel.

3. Materials and Methods

Experimental method consists in a combination of various devices to determine the thermal performance of the cook stoves. Thus, we use a GL-200 datalogger with an accuracy of ±5%, with four type K thermocouples to measure the evolution of temperatures at the level of the side walls of the cook stove and inside the stainless steel stockpot. The mass of the rice husk and the parboiled rice are weighed by a numerical scale of OHAUS-300 Series (weight 5 - 150 kg), with an accuracy of ±0.05 kg. The high temperature points on the surface of the cook stove are recorded by a Chauvin Arnoux Raycam infrared thermal camera with a temperature range of −20˚C to 600˚C. Finally, an ABB-EL3020 gas analyzer is used to determine the composition of the gases produced by the combustion of the rice husk. The methodological approach includes three steps. The first step consists of the ignition of the cook stove with the rice husk as fuel. This allows to verify the thermal combustion. The second step is to boil water from the heat produced by the combustion of the rice husk. The third step to test the paddy rice parboiling of with the vapor produced. The numerical method consists in solving Equations (7)-(12) by the Gauss Seidel algorithm.

4. Results and Discussions

The data extracted from the datalogger during our tests are presented in the form of figures. The curves of **Figure 2** show the surface temperature evolution of the burners. Thus, we note a maximum temperature of $T_{cu_1} = 304.78^{\circ}\mathrm{C}$ during at least 30 minutes of the buners. We vary the mass of the rice husk M = 5 - 10 kg in order to find a mass of average fuel to obtain a high temperature of the surface of the burners. Also, we contacted that the increase of the mass of the fuel doesn't necessarily involve a significant increase the surface temperature of the burners. Therefore, M = 7.15 kg is considered as the optimal mass to have a good combustion in the cook stove chamber.

The air flow evolution of circulating in the combustion chamber of the cook stove is represented by the curves in **Figure 3**. Thus, we note an air flow rate varies Q_m = 0.09112 $\mathrm{m^{-3}{\cdot}s^{-1}}$ to Q_m = 0.0839 $\mathrm{m^{-3}{\cdot}s^{-1}}$. This variation of the air flow is controlled by the ventilation system. It is motivated because we want to inject a

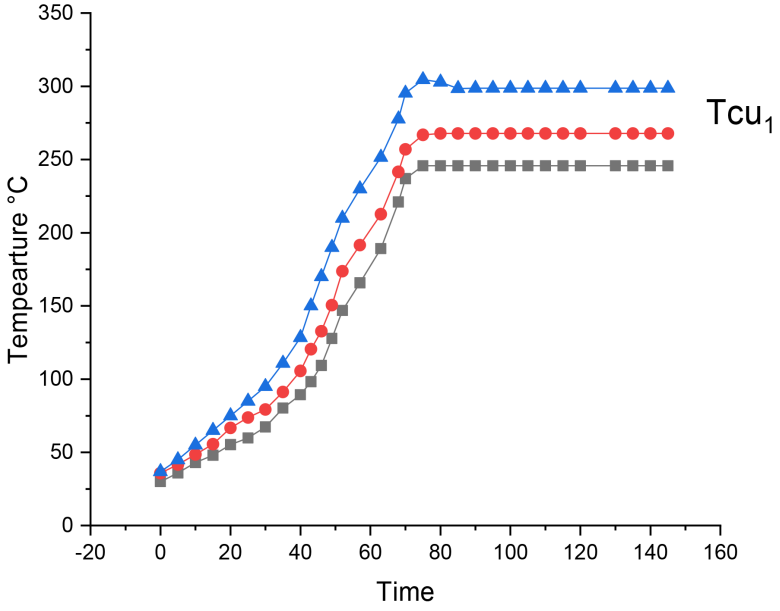

Figure 2. Surface temperature time evolution of burners of the cook stove.

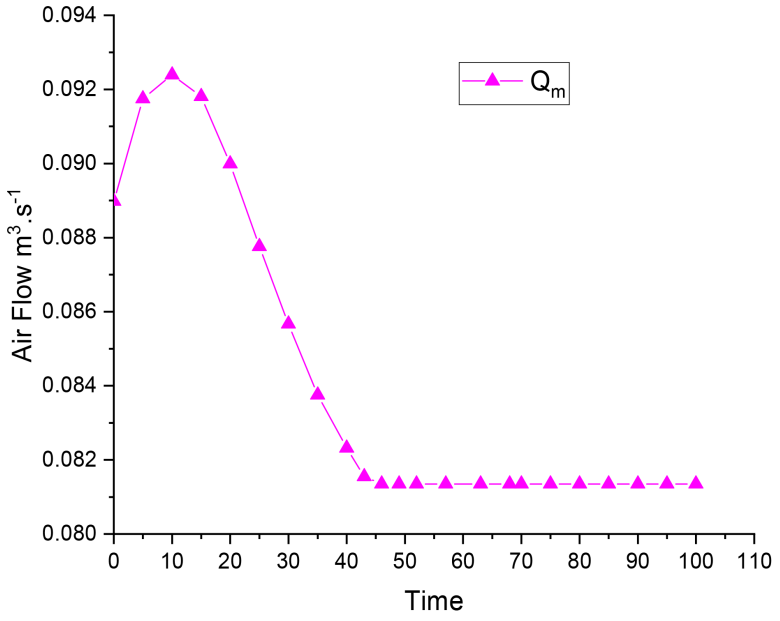

Figure 3. Air flow time evolution in combustion chamber.

precise air flow into the combustion chamber. A good combustion in the chamber allows to obtain a good temperature at the level of the burners.

We illustrate the surface temperature of the burners by the images of the Infrared Camera (IRC) of **Figure 4**, confirming the measured value of the temperature of the burners of the cook stove with the stainless steel stockpot at $T_{cu_1} = 304.78^{\circ}\mathrm{C}$ and without pot at $T_{cu_1} = 303.88^{\circ}\mathrm{C}$. The slight difference in temperature between $T_{cu_1} = 304.78^{\circ}\mathrm{C}$ and $T_{cu_1} = 303.88^{\circ}\mathrm{C}$ can be explained by the fact that the lower part of the stockpot reduces the effect of natural convection around the cook stove.

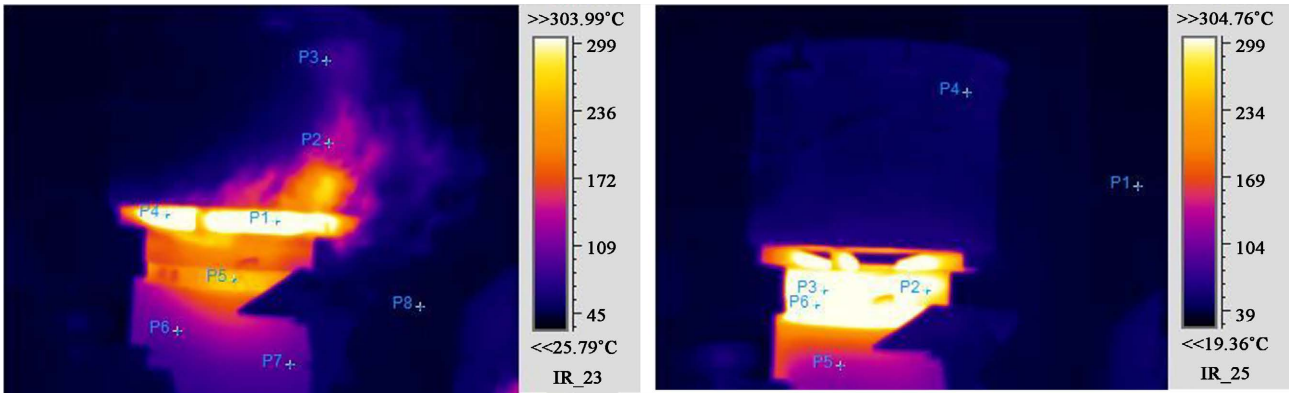

Figure 4. Camera infra-rouge image.

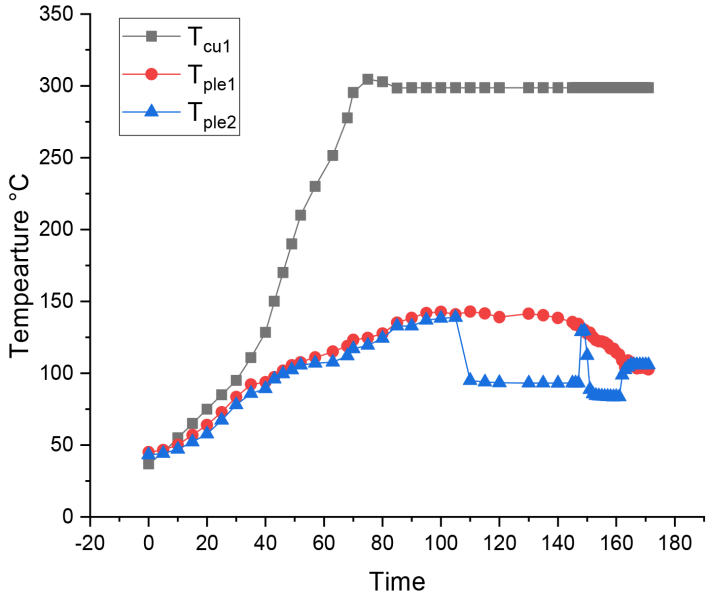

Figure 5. Surface temperature time evolution the burners and the vertical wall.

The external surfaces temperatures evolution the two vertical walls sides of the cook stove are $T_{ple_1} = 140.6^{\circ}\text{C}$ and $T_{ple_2} = 139.8^{\circ}\text{C}$ are presented by the curves of **Figure 5**. We notice that they are almost the same temperatures the two vertical walls. On the other hand, we observe two drops in temperature at the level of one of the walls respectively from $T_{ple_1} = 90.7^{\circ}\text{C}$ and to $T_{ple_1} = 80.6^{\circ}\text{C}$. These temperature drops can be explained by the fact that under the effect of the temperature, the k-type thermocouple has detached from the vertical wall of the cook stove during our tests. Also, we observe that both vertical walls of the cook stove lose almost the same temperature and this can be explained by their small thicknesses Ep = 2 mm of the black steel sheet. We note that the insulation absence inside the vertical walls contributes conductive heat transfer. Also, the average temperatures water and vapor is about 144.6˚C in the stainless steel sheet stockpot. This vapor temperature is favourable for paddy rice parboiling activities.

The curves in **Figure 6** show the composition of gases over the time of rice husk combustion. We observe the presence of carbon monoxide (CO), carbon

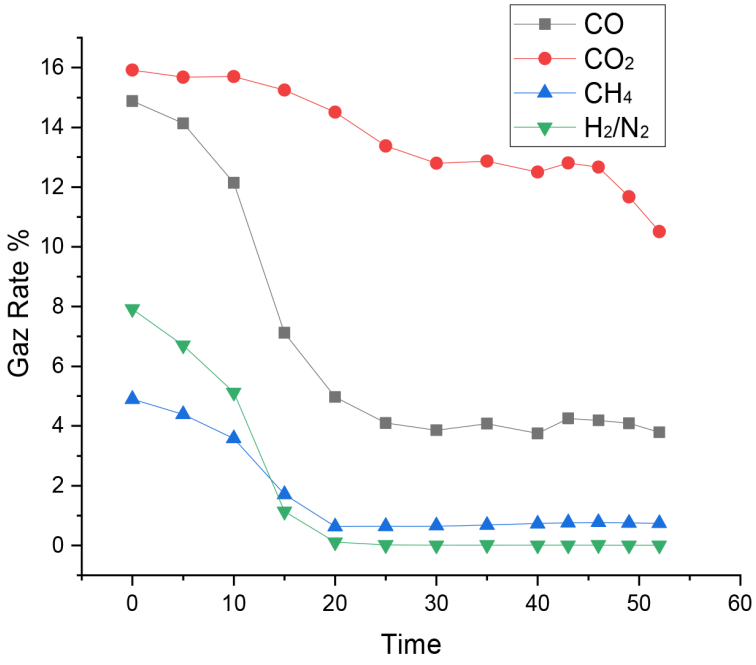

Figure 6. Gas combustion time evolution of rice husk.

dioxide (CO_2), methane (CH_4) and the ratio of Hydrogen to Nitrogen (H_2/N_2) with a predominance of CO_2. The average gas contents of CO_2, CO, CH_4 and H_2/N_2 are respectively 13.44%, 7.05%, 1.48% and 1.67%. We can see that these gas rates produced by the cook stove are not harmful to the health of users provided that the cook stove is used in a ventilated environment.

In order to compare the experimental tests results, we proceed to the numerical modeling of the cook stove prototype. Thus, the knowledge of the temperatures spatio-temporal distributions of the burners and the vertical walls is necessary to determine the thermal performances of the cook stove. Thus, we present the numerical results in the form of figures. The curves in **Figure 7** show the temperatures evolution of the external and internal wall surface of the cook stove. So, the calculated value is $T_{ple} = 144.55^{\circ}\text{C}$. Also, the **Figure 7** shows the temperature evolution of the burners surface. The simulated numerical value is $T_{cu_1} = 307.8^{\circ}\text{C}$. By symmetry, we present a one vertical wall.

The air flow evolution simulated of the in the combustion chamber of the cook stove is presented by the curves in **Figure 8**. Thus, an air flow $Q_m = 0.09258$ $m^{-3}{\cdot}s^{-1}$ is observed. At the beginning of the operation, the air flow rate is high $Q_m = 0.09258$ $m^{-3}{\cdot}s^{-1}$ after about 30 min of operation the air flow rate is reduced to $Q_m = 0.08288$ m^{-3} This is due to the fact that a high air flow rate leads to a faster consumption of the rice husk. Also, we contacted that if $M = 10$ kg the maximum value of the fuel, there is a bad combustion within the combustion chamber generating a carbonization of the rice husk. This carbonization leads to an important gaseous emission and especially the appearance of tar, which can cause important damage to the ventilation system and the cook stove users.

The quantitative analysis of the different operating parameters of the cook

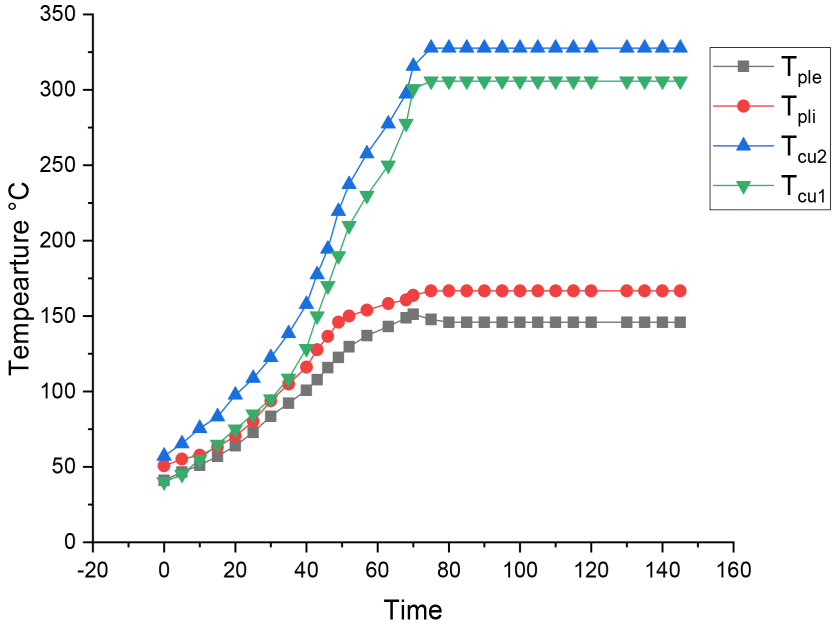

Figure 7. Temperature space-time evolution of the burners and the vertical walls.

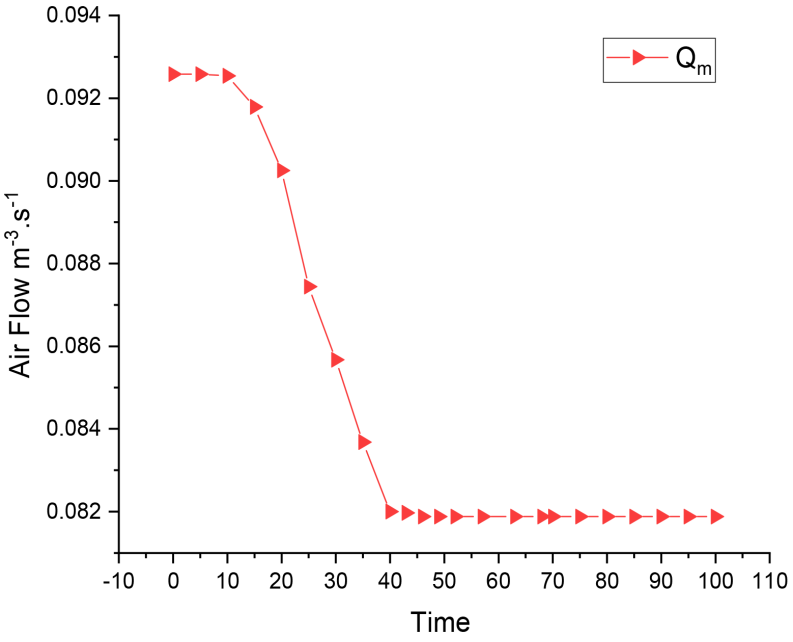

Figure 8. Air flow space-time evolution circulate in the combustion chamber.

stove shows that the measured values and those simulated are in good agreement. The difference is estimated at 5%. So, the thermal performance of the cook stove is calculated by the ratio of the energy required to bring the water to boiling point to the energy produced by the cook stove in operation, taking into account the latent heat and the mass of water evaporated. This ratio indicates an average efficiency is η = 46.6%. This yield indicates an acceptable operation of the cook stove. The power developed by the cook stove the ratio of the energy produced over time. This power is 5.96 kW≈ 6 kW.

5. Conclusions

At the end of this experimental study of the thermal performances of the cook stove, we show that the temperatures of the burners and the two vertical walls influence the thermal performances. During the tests we determined the mass M = 7.15 kg is the optimal mass of the rice husk, for a good combustion in the combustion chamber. Thus, for air flow rate varying from Q_m = 0.09112 $m^{-3}{\cdot}s^{-1}$ to Q_m = 0.0839 $m^{-3}{\cdot}s^{-1}$, burners temperature is $T_{cu_1} = 304.78^{\circ}C$ and the temperature of the vertical wall $T_{ple_1} = 140.6^{\circ}C$. The water temperature and vapor generated in the stockpot is about 144.6˚C.

The gaseous emissions from the combustion of the rice husk are composed of carbon dioxide (CO_2); carbon monoxide CO; methane CH_4 and the ratio of hydrogen to nitrogen H_2/N_2. The proportion of these gases is respectively 13.44%; 7.05%; 1.48% and 1.67%. These proportions don't represent any major risk for rice parboilers. Following these experimental tests, we have developed a mathematical model to simulate numerically the thermal behavior of the cook stove. We obtained the surface temperature of the burners $T_{cu_1} = 307.8^{\circ}C$, the vertical walls temperature is T_{ple} = 144.55˚C and an air flow varying from Q_m = 0.09258 $m^{-3}{\cdot}s^{-1}$ to Q_m = 0.08288 $m^{-3}{\cdot}s^{-1}$. These results show that the vertical walls of the cook stove lose heat. Despite these heat losses, the cook stove is still very interesting for paddy rice parboiling. It can significantly improve the quantity of paddy rice. Finally, the average thermal efficiency is η = 46.6% and the power developed by the furnace is ≈6 kW. Some recommendations have been made to improve the cook stove for paddy rice parboiling.

Acknowledgements

The authors wish to thank the Project Centers for Green Innovations in the Agrifood Sector in Bobo-Dioulasso and German cooperation Giz for financial support.

Conflicts of Interest

The authors declare no conflicts of interest regarding the publication of this paper.

References

[1] Visser, P. (2005) The Testing of Cookstoves: Data of Water-Boiling Tests as a Basis to Calculate Fuel Consumption. *Energy for Sustainable Development*, **9**, 16-24. https://doi.org/10.1016/S0973-0826(08)60479-2

[2] Modi, K. and Upadhyay, D.S. (2021) Experimental Investigations and Thermal Analysis of a Natural Draft Improved Biomass Cookstove with Different Air Conditions. *IOP Conference Series*: *Materials Science and Engineering*, **1146**, Article ID: 012010. https://doi.org/10.1088/1757-899X/1146/1/012010

[3] Parajuli, A., Agrawal, S., Tharu, J.K., Kamat, A.K., Jha, A.K. and Darlami, H.B. (2019) A Simplified Model for Understanding the Performance of Two-Pot Enclosed Mud Cookstove. *Clean Energy*, **3**, 288-306. https://doi.org/10.1093/ce/zkz020

[4] Sagouong, J.M. and Tchuen, G. (2018) Mathematical Modelling of Traditional Stoves Using the Thermal Network Approach. *International Journal of Engineering Trends and Technology*, **58**, 1-9. https://doi.org/10.14445/22315381/IJETT-V58P201

[5] Gandigude, A. and Nagarhalli, M. (2018) Simulation of Rocket Cook-Stove Geometrical Aspect for Its Performance Improvement. *Materials Today*: *Proceedings*, **5**, 3903-3908. https://doi.org/10.1016/j.matpr.2017.11.645

[6] CILSS (2004) Etude de consommation de combustible domestique. PREDAS. 55 p.

[7] Caron, F. (2010) La dynamique de l'innovation: Changement technique et changement social. Edition Gallimard, 469 p.

[8] Boggavarapu, P., Ray, B. and Ravikrishna, R.V. (2014) Thermal Efficiency of LPG and PNG Fired Burners: Experimental and Numerical Studies. *Fuel*, **116**, 709-715. https://doi.org/10.1016/j.fuel.2013.08.054

[9] Arora, P., Jain, S. and Sachdeva, K. (2014) Laboratory Based Assessment of Cookstove Performance Using Energy and Emission Parameters for North Indian Cooking Cycle. *Biomass and Bioenergy*, **69**, 211-221. https://doi.org/10.1016/j.biombioe.2014.07.012

[10] Arora, P., Das, P., Jain, S. and Kishore, V.V.N. (2014) A Laboratory Based Comparative Study of Indian Biomass Cook Stove Testing Protocol and Water Boiling Test. *Energy for Sustainable Development*, **21**, 81-88. https://doi.org/10.1016/j.esd.2014.06.001

[11] Bailis, R., Berrueta, V., Chengappa, C., Dutta, K., Edwards, R., Masera, O., Still, D. and Smith, K.R. (2007) Performance Testing for Monitoring Improved Biomass Stove Intervent Ions: Experiences of the Household Energy and Health Project. *Energy for Sustainable Development*, **11**, 57-70. https://doi.org/10.1016/S0973-0826(08)60400-7

[12] Boafo-Mensah, G., Darkwa, K.M. and Laryea, G. (2020) Effect of Combustion Chamber Material on the Performance of an Improved Biomass Cookstove. *Case Studies in Thermal Engineering*, **21**, Article ID: 100688. https://doi.org/10.1016/j.csite.2020.100688

[13] Grimsby, L.K., Rajabu, H.M. and Treiber, M.U. (2016) Multiple Biomass Fuels and Improved Cookstoves from Tanzania Assessed with the Water Boiling Test. *Sustainable Energy Technologies and Assessments*, **14**, 63-73. https://doi.org/10.1016/j.seta.2016.01.004

[14] Gupta, A., Mulukutla, A.N.V., Gautam, S., TaneKhan, W., Waghmare, S.S. and Labhasetwar, N.K. (2020) Development of a Practical Evaluation Approach of a Typical Biomass Cookstove. *Environmental Technology & Innovation*, **17**, Article ID: 100613. https://doi.org/10.1016/j.eti.2020.100613

[15] Jagger, P. and Das, I. (2018) Implementation and Scale-Up of a Biomass Pellet and Improved Cook Stove Enterprise in Rwanda. *Energy for Sustainable Development*, **46**, 32-41. https://doi.org/10.1016/j.esd.2018.06.005

Nomenclature

T = Temperature (˚C)
t = Time (s)
S = Surface (m^2)
S_0 = Section (m^2)
λ = Thermal conductivity ($W \cdot m^{-1} \cdot K^{-1}$)
L = Length (m)
V = Velocity ($m \cdot s^{-1}$)
Ep = Thicknesses (m)
M = The mass of the section (kg)
Cp = Calorific Capacity ($J \cdot kg^{-1} \cdot K^{-1}$)
hr = Radiation transfer coefficient
hc = Transfer coefficients of natural convection ($W \cdot m^{-2} \cdot K^{-1}$)
Q_m = Airflow volume ($m^3 \cdot s^{-1}$)
Δt = Step time (s)
F = Geometric Form factor
Pu = Useful flow density($W \cdot m^2$)

Index

ple = External surface
pli = Internal surface
a = Air in combustion chamber
fon = Lower temperature
cu_1 = External surface
cu_2 = Internal surface
amb = Ambient
sol = Soil